ラットの作成c) パーキンソン病モデル動物における細胞移植の有効性・機能回復効果・安全性の検証を行った。今回はa)およびb)の 2 項目の結果と、c)の項目については現在の進捗状況を報告する。

(2 - 1)パーキンソン病治療に向けて

a) ドーパミン神経細胞への分化誘導法の確立

SHEDのドーパミン神経細胞への分化誘導はstep1およびstep2の2段階で行った。誘導前およびstep1では免疫染色でTH（チロシン水酸化酵素、ドーパミンの産生に関与する）マーカーの発現は認められなかったが、step2では高率でマーカーの発現が認められた。(Fig1) このことから、SHEDはstep2においてTHマーカー陽性のドーパミン神経細胞に分化することがわかった。

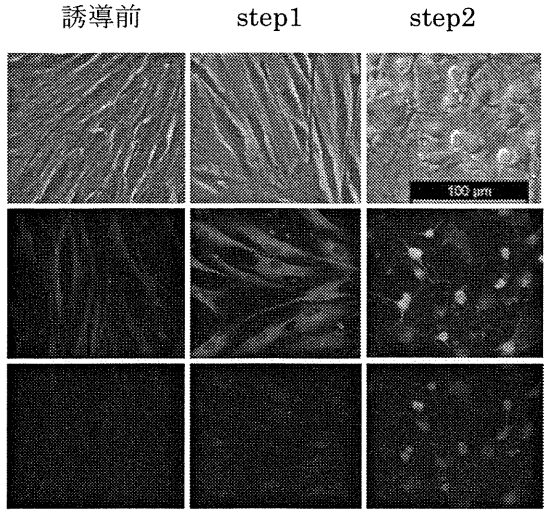

Fig1　誘導前、step1、step2のドーパミン神経細胞への分化(488:TH,546:Tuj1,DAPI)

ドーパミン神経細胞への分化誘導効率は、TH陽性細胞の割合(Fig2)と細胞生存率（トリパンブルー染色で死細胞を染色）(Fig3)により評価した。

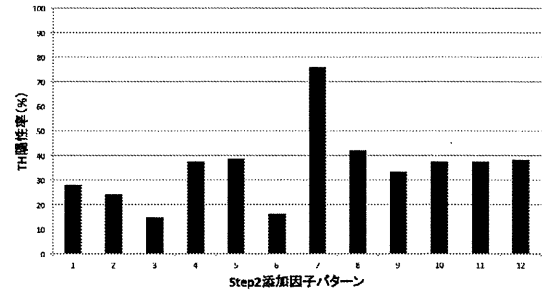

Fig2　分化誘導後のTH陽性細胞の割合(n=2)

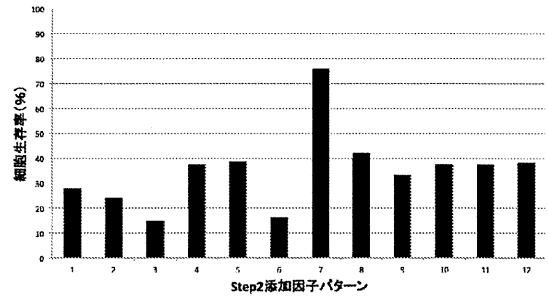

Fig3　分化誘導後の細胞生存率(n=2)

TH陽性細胞の割合および細胞生存率は、step2培養でBDNFを添加したもの（パターン7）が最も高率であった。このことから、step2においてBDNFを添加する方法が、SHEDの最も効率の良い分化誘導法であることがわかった。

b) パーキンソン病モデル動物(ラットまたはマウス)の作成

c) パーキンソン病モデル動物における細胞移植の有効性・機能回復効果・安全性の検証

step2においてBDNFを添加する方法で分化誘導したSHEDをパーキンソンモデルラットの障害側の線条体に移植し、メタンフェタミン投与による回転運動により行動を評価した。その結果、3匹のラットで移植の1週間後から

回転運動が減少し、行動改善が認められた。(Fig4)

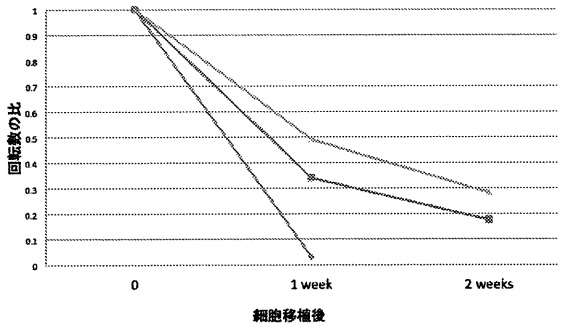

Fig4　分化誘導細胞移植後のパーキンソンモデルラットの回転数(n=3)

今後はより多くのパーキンソンモデルラットを作製して細胞移植による行動改善効果を確認すると共に、組織学的解析を進める予定である。

D. 考察

歯髄幹細胞の神経分化能を検討したところ、SHED、DPSCともに90%以上が神経幹細胞・幼弱神経細胞・アストロサイト・未成熟オリゴデンドロサイトのマーカーを共発現していた。その一方で、成熟型神経細胞や成熟オリゴデンドロサイトのマーカーは発現していなかった。このことから、歯髄幹細胞は神経細胞のみならず、アストロサイトやオリゴデンドロサイトへの分化能も持ち合わせた、未成熟状態にある、ユニークな細胞集団であることが見出された。また、歯髄幹細胞は神経分化誘導にも正常な応答能を示した。他の体性幹細胞である骨髄間葉系幹細胞(BMSCs)や線維芽細胞(FBs)と比較すると、歯髄幹細胞はSHED、DPSCともにGDNF、BDNF、CNTFといった神経栄養因子群を高率に発現していた。GDNFはドーパミンの取り込みと中脳神経細胞の生存および形態学的分化を特異的に促進することが知られており、このことから歯髄幹細胞のほうが骨髄間葉系幹細胞と比較してパーキンソン病治療応用に有用であると推測される。またSHEDは骨髄間葉系幹細胞と比較して、有意にGABA作動性神経細胞への分化に必須である Ptf1aの発現が高かったことから、脊髄小脳変性症治療にも歯髄幹細胞のほうが有用であることが推察される。パーキンソン病治療のため、高効率でドーパミン神経細胞を分化誘導できる条件を各種検討した結果、step1およびstep2の2段階で培養し、step1ではbFGFとEGFを添加することで成熟型神経細胞に分化し、step2でさらにshhやBDNFなどの添加因子を加えることでTH陽性のドーパミン神経細胞に分化誘導できることがわかった。なかでもstep2でBDNFを添加する方法が、最もTH陽性細胞への分化率および細胞生存率が高く、SHEDの最も効率の良い分化誘導法であることがわかった。また、この方法で分化誘導したSHEDをパーキンソンモデルラットに移植し、行動改善が認められた。

今後はドーパミン産生細胞への分化を遺伝子レベルでも評価すると共に、BDNFの添加により分化効率が高まる作用機序についても検討する予定である。また、より多くのパーキンソンモデル動物に分化した細胞を移植してその治療効果を実証し、組織学的な解析も進め、

歯髄幹細胞の移植治療への実用化の可能性を検討していく予定である。

E. 結論

我々はSHEDを高効率でドーパミン神経細胞を分化誘導する方法を見出した。また、動物

実験によりSHEDは神経疾患治療に有用な細胞源であることが強く示唆された。今後さらに解析を進め、SHEDを用いた神経再生治療の実用化を目指す。

F .健康危険情報

本研究において、国民の生命・健康に重大な影響を及ぼす事項は発生していない。

G.研究発表

1.論文発表　なし

2.学会発表　なし

H.知的財産権の出願・登録状況(予定を含む)

1.特許出願

2.実用新案登録　なし

3.その他　なし

研究成果の刊行に関する一覧表

雑誌

発表者氏名	論文タイトル名	発表誌名	巻号	ページ	出版年
Sugiyama, M., Iohara, K., Wakita, H., Hattori, H., Ueda, M., Matsushita, K., Nakashima, M.	Dental Pulp-Derived CD31 −/CD146 − Side Population Stem/Progenitor Cells Enhance Recovery of Focal Cerebral Ischemia in Rats.	Tissue Eng Part A	Vol.17 No.9-10	1303-0311	2011
Kiyoshi Sakai, Akihito Yamamoto, Kohki Matsubara, Shoko Nakamura, Mami Naruse, Mari Yamagata, Kazuma Sakamoto, Ryoji Tauchi, Norimitsu Wakao, Shiro Imagama, Hideharu Hibi, Kenji Kadomatsu, Naoki Ishiguro, Minoru Ueda	Human dental pulp-derived stem cells promote locomotor recovery after complete transection of the rat spinal cord by multiple neuro-regenerative mechanisms	The Journal of Clinical Investigation	Vol.122 No.1	80-90	2011
Ebisawa K, Kato R, Okada M, Sugimura T, Latif MA, Hori Y, Narita Y, Ueda M, Honda H, Kagami H.	Gingival and dermal fibroblasts: their similarities and differences revealed from gene expression.	Journal of Bioscience and Bioengineering	Vol.111 No.3	255-258	2011
Masahito Fujio, Akihito Yamamoto, Yuji Ando, Ryutaro Shohara, Kazuhiko Kinoshita, Tadashi Kaneko, Hideharu Hibi, Minoru Ueda	Stromal cell-derived factor-1 enhances distraction osteogenesis-mediated skeletal tissue regeneration through the recruitment of endothelial precursors	Bone	Vol.49	693-700	2011
Hideharu Hibi, Minoru Ueda	Supraperiosteal Transport Distraction Osteogenesis for Reconstructing a Segmental Defect of the Mandible	American Association of Oral and Maxillofacial Surgeons Journal Oral Maxillofac Surg	Vol.69	742-746	2011

Masayuki Ikeno, Hideharu Hibi, Kazuhiko Kinoshita, Hisashi Hattori, Minoru Ueda,	Effects of Self-Assembling Peptide Hydrogel Scaffold on Bone Regeneration with Recombinant Human Bone Morphogenetic Protein-2	Oral Craniofac Tissue Eng	Vol.1	91–97	2011
Masayuki Ikeno, Hideharu Hibi, Kazuhiko Kinoshita, Hisashi Hattori, Minoru Ueda	Effects of the Permeability of Shields with Autologous Bone Grafts on Bone Augmentation	Oral Craniofac Tissue Eng	Vol.1	198-204	2011
Tomoyuki Kohgo, Yoichi Yamada, Kenji Ito, Akihiro Yajima, Ryoko Yoshimi, Kazuto Okabe, Shunsuke Baba, Minoru Ueda	Bone Regeneration with Self-Assembling Peptide Nanofiber Scaffolds in Tissue Engineering for Osseointegration of Dental Implants	Int. J Periodontics Restorative Dent	Vol.31	e9-e26	2011
Yudai Nishino, Katsumi Ebisawa, Yoichi Yamada, Kazuto Okabe, Yuzuru Kamei, Minoru Ueda,	Human Deciduous Teeth Dental Pulp Cells With Basic Fibroblast Growth Factor Enhance Wound Healing of Skin Defect	J Craniofac Surg	Vol.22	438-442	2011
Yasuhiro Okamoto, Hideo Tateishi, Kazuhiko Kinoshita, Shuhei Tsuchiya, Hideharu Hibi, and Minoru Ueda	An Experimental Study of Bone Healing Around the Titanium Screw Implants in Ovariectomized Rats: Enhancement of Bone Healing by Bone Marrow Stromal Cells Transplantation	Implant Dentistry	Vol.20 No.3	236-245	2011
Fumihito Sato, Isao Oze, Daisuke Kawakita, Noriyuki Yamamoto, Hidemi Ito, Satoyo Hosono, Takeshi Suzuki, Takakazu Kawase, Hiroki Furue, Miki Watanabe, Shunzo Hatooka, Yasushi Yatabe, YasuhisaHasegawa, Masayuki Shinoda,	INVERSE ASSOCIATION BETWEEN TOOTHBRUSHING AND UPPER AERODIGESTIVE TRACT CANCER RISK IN A JAPANESE POPULATION	HEAD & NECK–	Vol.33 No.11	1628-37	2011

Minoru Ueda, Kazuo Tajima, Hideo Tanaka, Keitaro Matsuo					
Masayuki Tamari, Yudai Nishino, Noriyuki Yamamoto, Minoru Ueda	Acceleration of Wound Healing with Stem Cell-Derived Growth Factors	Oral & Craniofacial Tissue Engineering	Vol.1	181-187	2011
RYU WADAGAKI, DAIKI MIZUNO, AIKA YAMAWAKI-OGATA, MAKOTO SATAKE, HIROAKI KANEKO, SUMITAKA HAGIWARA, NORIYUKI YAMAMOTO, YUJI NARITA, HIDEHARU HIBI, MINORU UEDA	Osteogenic Induction of Bone Marrow-Derived Stromal Cells on Simvastatin-Releasing, Biodegradable, Nano- to Microscale Fiber Scaffolds	Annals of Biomedical Engineering,	Vol.39 No.7,	1872 - 1881	2011
光藤健司、岩井俊憲、光永幸代、小栗千里、小泉敏之、來生知、廣田誠、玉利正之、山本憲幸、上田実、藤内祝	進行口腔癌に対する逆行性超選択的動注化学放射線療法	頭頸部癌	37巻 3号	386-389	2011

TISSUE ENGINEERING: Part A
Volume 17, Numbers 9 and 10, 2011

DOI: 10.1089/ten.tea.2010.0306

Dental Pulp-Derived CD31$^-$/CD146$^-$ Side Population Stem/Progenitor Cells Enhance Recovery of Focal Cerebral Ischemia in Rats

Masahiko Sugiyama, D.D.S.,[1,2] Koichiro Iohara, Ph.D.,[1] Hideaki Wakita, Ph.D.,[3] Hisashi Hattori, Ph.D.,[2] Minoru Ueda, Ph.D.,[2] Kenji Matsushita, Ph.D.,[1] and Misako Nakashima, Ph.D.[1]

Regenerative therapy using stem cells is a promising approach for the treatment of stroke. Recently, we reported that CD31$^-$/CD146$^-$ side population (SP) cells from porcine dental pulp exhibit highly vasculogenic potential in hindlimb ischemia. In this study, we investigated the influence of CD31$^-$/CD146$^-$ SP cells after transient middle cerebral artery occlusion (TMCAO). Adult male Sprague-Dawley rats were subjected to 2 h of TMCAO. Twenty-four hours after TMCAO, CD31$^-$/CD146$^-$ SP cells were transplanted into the brain. Motor function and infarct volume were evaluated. Neurogenesis and vasculogenesis were determined with immunochemical markers, and the levels of neurotrophic factors were assayed with real-time reverse transcription–polymerase chain reaction. In the cell transplantation group, the number of doublecortin-positive cells increased twofold, and the number of NeuN-positive cells increased eightfold, as compared with the control phosphate-buffered saline group. The vascular endothelial growth factor level in the ischemic brain with transplanted cells was 28 times higher than that in the normal brain. In conclusion, CD31$^-$/CD146$^-$ SP cells promoted migration and differentiation of the endogenous neuronal progenitor cells and induced vasculogenesis, and ameliorated ischemic brain injury after TMCAO.

Introduction

Several preclinical studies have provided evidence that transplanted stem cells have therapeutic potential in the treatment of stroke.[1] Stem cells have the capability to migrate to areas of injury and secrete neuroprotective factors to induce neurogenesis.[2] In the adult mammalian brain, neurogenesis persists in certain distinct regions of the central nervous system such as the subventricular zone (SVZ) and the dentate gyrus of the hippocampus.[3] It has been reported that transplanting differentiated neural stem cells isolated from dental pulp improved motor disability and reduced infarct volume.[4] However, the influence of transplanting stem/progenitor cells isolated from dental pulp in cerebral ischemia has not been elucidated. Recently, we reported that CD31$^-$/CD146$^-$ side population (SP) cells containing stem/progenitor cells from porcine dental pulp exhibit highly vasculogenic potential *in vitro* and promote revascularization in hindlimb ischemia.[5] In the present study, we investigated the effects of these cells on neurogenesis and vasculogenesis in a cerebral ischemia model in a rat. In addition, the effects on the motor dysfunction and infarct volume were evaluated after transient middle cerebral artery occlusion (TMCAO).

Materials and Methods

Isolation of CD31$^-$/CD146$^-$ SP cells

CD31$^-$/CD146$^-$ SP and CD31$^+$/CD146$^-$ SP cells were isolated from porcine tooth germ, as described previously.[5] CD31$^-$/CD146$^-$ SP cells were cultured in endothelial basal medium-2 (EBM-2, single quots cc–4176) with 10 ng/mL insulin-like growth factor 1 (IGF1), 10 ng/mL epidermal growth factor (EGF), and 10% fetal bovine serum (FBS). CD31$^+$/CD146$^-$ SP cells were cultured in EBM-2 with 10 ng/mL bFGF, 10 ng/mL vascular endothelial growth factor (VEGF), 138 nM hydrocortisone, 0.09 mg/mL heparin, 50 μg/mL ascorbic acid, and 10% FBS. They were routinely subcultured up to 70% confluence under identical conditions.

Cerebral ischemia model

All animal experiments were approved by the Institutional Animal Care and Use Committee (National Center for the Geriatrics and Gerontology). Adult male Sprague-Dawley rats (Japan SLC, Inc.) weighing 300–400 g were used. Animals were initially anesthetized with 5% isoflurane (Abbott Laboratories) and maintained under anesthesia with 1.5% isoflurane in a mixture of 70% N_2O and 30% O_2. Rectal

[1]Department of Oral Disease Research, National Center for Geriatrics and Gerontology, Research Institute, Obu, Aichi, Japan.
[2]Department of Oral and Maxillofacial Surgery, Laboratory Medicine, Nagoya University Graduate School of Medicine, Nagoya, Japan.
[3]Department of Vascular Dementia Research, National Center for Geriatrics and Gerontology, Research Institute, Obu, Aichi, Japan.

temperature was maintained at 37°C±0.5°C on a heating pad. Focal cerebral ischemia was induced by TMCAO with 2 h.[6] A 4-0 monofilament nylon suture (Shirakawa) with the tip rounded by flame heating and silicone (KE-200; Shin-Etsu Chemical) was advanced from the external carotid artery into the internal carotid artery until it blocked the origin of the MCA. Two hours after occlusion, reperfusion was performed by withdrawal of the suture. The regional cerebral blood flow of the MCA territory was measured using a laser-Doppler flowmeter (Omega FLO-N1; Omega Wave, Inc.) after occlusion. The response was considered positive and included only if the reduction in regional cerebral blood flow was >70%.

Transplantation

Twenty-four hours after TMCAO (day 0), the rats were again anesthetized with sodium pentobarbital (Schering-Plough) (0.25 mL/kg, intraperitoneally) and maintained under anesthesia with 1.5% isoflurane in a mixture of 70% N_2O and 30% O_2. Animals were randomly divided into three groups: (I) $CD31^-/CD146^-$ SP cell transplantation group ($n=24$, day 3 sacrificed=6, day 9 sacrificed=7, day 21 sacrificed=11), (II) unfractionated pulp cell transplantation group ($n=4$, used for motor function), and (III) vehicle alone (phosphate-buffered saline [PBS]) group ($n=20$, day 3 sacrificed=6, day 9 sacrificed=5, day 21 sacrificed=9). The infarction site was targeted for transplantation at the striatum of the following coordinates: 1.0 mm rostral to the bregma, 6.0 mm lateral to the midline, 5.0 mm ventral to the dura (Fig. 1A, B). Subsequently, 1×10^6 $CD31^-/CD146^-$ SP cells or unfractionated pulp cells at the fifth to seventh passage after labeling with 1,1-dioctadecyl-3,3,3,3 tetramethylindocarbocyanine perchlorate (DiI; Sigma), and removing all added factors into each medium were diluted with 2 μL of PBS, and were transplanted by Hamilton microsyringe (Hamilton). The control group consisted of an equal volume of PBS injected into the same site.

Immunohistochemistry

At day 3 or 21 after injection, the rat was transcardially perfused with 4% paraformaldehyde solution (Nakarai Tesque). The brain was removed and postfixed in paraformaldehyde. The following day, it was immersed in 30% sucrose solution. Twelve-micrometer-thick coronal sections were cut on a cryostat. For immunohistochemistry, the sections were preincubated in blocking solution (PBS containing 5% normal serum of the species in which the secondary antibody was raised) for 2 h at room temperature, and incubated with primary antibodies diluted for 1 h at room temperature. The primary antibodies were as follows: neuronal progenitor cells (NPC) marker, rabbit anti-doublecortin (1:50; Abcam, Inc.); neuron marker, rabbit anti-neurofilament H (1:200; Chemicon) and mouse anti-NeuN (anti-neuronal nuclei, 1:500; Chemicon); endothelial cell marker, mouse anti-RECA1 (rat endothelial cell antigen; Monosan); apoptosis marker, rabbit anti-cleaved caspase-3 (1:50; Cell Signaling Technology, Inc.); and VEGF marker, rabbit anti-VEGF (VEGF [P-20]: sc-1836; Santa Cruz Biotech). After washing, sections were incubated for 1 h at room temperature with secondary antibodies (on day 21, for neurofilament H/doublecortin, Donkey anti-rabbit IgG FITC [1:400; Jackson ImmunoResearch]; for NeuN/RECA1, Goat anti-mouse IgG FITC [1:200; MP Biomedicals]; and for VEGF, rabbit anti-goat IgG-HRP [1:400; Invitrogen Corporation]. On day 3, for cleaved caspase-3, goat anti-rabbit IgG-HRP [1:400; Invitrogen] and for VEGF, rabbit anti-goat IgG-HRP [1:400; Invitrogen]). The sections with HRP-conjugated secondary antibodies were incubated in anti-fluorescein-HRP (1:400; TSA™ Fluorescence Systems; PerkinElmer) for 7 min at room temperature. Adjacent sections were used as negative controls. In the control sections, all procedures were processed in the same manner except that the primary antibodies were omitted. To identify migration of NPC from SVZ, we observed the cryosections on days 9 and 21 with anti-doublecortin on fluorescence microscope (BZ-9000; Keyence) and BZ-HIC (Keyence).

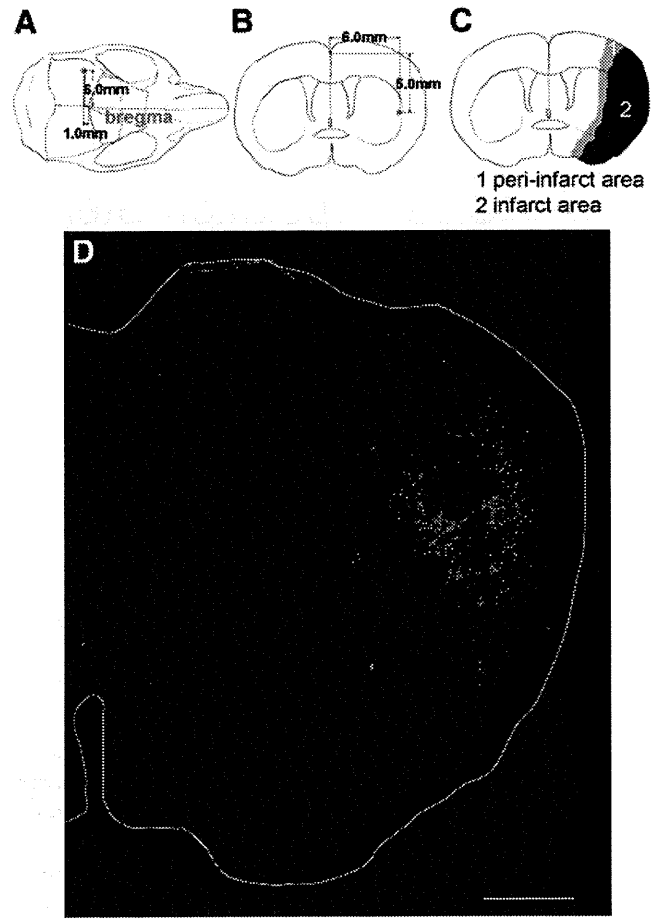

FIG. 1. **(A)** Overhead and **(B)** coronal view of the injection site. **(C)** The peri-infarct area. Peri-infarct area (gray), infarct core (black). **(D)** DiI-labeled transplanted $CD31^-/CD146^-$ SP cells (red) migrated from the original injection site to the peri-infarct area in the cortex and striatum. White outline is the outer circumference of brain. Scale bar = 1000 μm. SP, side population. DiI, 1,1-dioctadecyl-3,3,3,3 tetramethylindocarbocyanine perchlorate. Color images available online at www.liebertonline.com/tea

Statistical analyses of the density of cells

The density of NPCs, neurons, endothelial cells, and apoptotic cells in the peri-infarct area (Fig. 1C) and the contralateral region in the $CD31^-/CD146^-$ SP cell transplantation group and PBS groups were determined. In all groups (PBS group, $CD31^-/CD146^-$ SP cell transplantation group,

TABLE 1. PORCINE PRIMERS FOR REAL-TIME REVERSE TRANSCRIPTION–POLYMERASE CHAIN REACTION AND *IN SITU* HYBRIDIZATION

Gene		*5′ DNA sequence 3′*	*Product size (bp)*	*Accession no.*
r.β-actin	Forward	AAGTACCCCATTGAACACGG	257	NM_031144
	Reverse	ATCACAATGCCAGTGGTACG		
p.β-actin	Forward	CTGGGGCCTAACGTTCTCAC	198	BI118314
	Reverse	GTCCTTTCTTCCCCGATGTT		
VEGF	Forward	ATGGCAGAAGGAGACCAGAA	224	MN_214084
	Reverse	ATGGCGATGTTGAACTCCTA		
BDNF	Forward	TTCAAGAGGCCTGACATCGT	180	MN_214259
	Reverse	AGAAGAGGAGGCTCCAAAGG		
NGF	Forward	TGGTGTTGGGAGAGGTGAAT	210	L31889
	Reverse	CCGTGTCGATTCGGATAAA		
GDNF	Forward	ACGGCCATACACCTCAATGT	144	GU229658
	Reverse	CCGTCTGTTTTTGGACAGGT		

BDNF, brain-derived neurotrophic factor; GDNF, glial cell line-derived neurotrophic factor; NGF, nerve growth factor; VEGF, vascular endothelial growth factor.

and contralateral group, $n=3$), each five sections at every 120-μm were stained with doublecortin, NeuN, RECA1, and cleaved caspase-3. The microscopic images were scanned and five typical frames (0.49 mm^2) were measured for each section. Thus, 75 frames on an average were determined per group. The positively stained area relative to total area (7.41 mm^2) was statistically analyzed using a Dynamic cell count, BZ-HIC (Keyence).

Real-time reverse transcription–polymerase chain reaction

Total RNA on cryosamples was extracted using Trizol (Invitrogen) from the area of the DiI-positive cells observed in the section. First-strand cDNA syntheses were performed from total RNA by reverse transcription with ReverTra Ace-α (Toyobo). Real-time reverse transcription–polymerase chain reaction (RT-PCR) amplifications were performed at 95°C for 10 s, at 62°C for 15 s, and at 72°C for 8 s using the porcine-specific primers *VEGF*. The specificity of the primers to porcine was confirmed by no amplification of the first-strand cDNA from rats with normal brains. The RT-PCR products were subcloned into a pGEM-T Easy vector (Promega) and confirmed by DNA sequencing based on published cDNA sequences. Gene expression of the transplanted cells in the infarct area was compared with that in the porcine normal brain tissue and that in transplanted cells in the normal brain after normalizing with β-actin.

In situ *hybridization*

Neurotrophic factors expressed in $CD31^-/CD146^-$ SP cells were examined with *in situ* hybridization in cryosections on day 21. Porcine cDNA of *VEGF* (224 bp), glial cell line-derived neurotrophic factor (*GDNF*; 144 bp), brain-derived neurotrophic factor (*BDNF*;180 bp), and nerve growth factor (*NGF*; 210 bp) were linearized with *Nco*I, *Spe*I, *Nco*I, and *Spe*I, respectively, for anti-sense probes, and linearized with *Spe*I, *Nco*I, *Spe*I, and *Nco*I, respectively, for sense probes. The *VEGF* probe was constructed from plasmids after subcloning the PCR products using the same primers designed for real-time RT-PCR. The *GDNF*, *BDNF*, and *NGF* probes were also constructed in same way as the *VEGF* probe. Since a published porcine *GDNF* sequence was not available, human primers for *GDNF* (forward 5′-TATGGGATGTCGT GGCTGT-3′, reverse 5′-TCCACACCTTTTAGCGGAAT-3′) were used for cDNA subcloning of porcine *GDNF* (630 bp). The design of the oligonucleotide primers (Table 1) was based on both published porcine cDNA sequences and the newly cloned cDNA sequence of the porcine *GDNF*. The four probes were labeled with DIG (Invitrogen) and the DIG signals were detected with TSA system FITC-conjugated tyramide (Invitrogen).

Migration, proliferation, and anti-apoptotic assays

At 50% confluence, the culture medium was switched to serum-free EBM-2. The conditioned medium (CM) from $CD31^-/CD146^-$ SP cells, $CD31^+/CD146^-$ SP cells, and unfractionated pulp cells were collected after 48 h.

For migration assay, modified Boyden chamber assays were performed with polyethylene terephthalate membrane (BD Bioscience) in a 24-well plate (BD Bioscience). SHSY5Y cells (Sanyo Chemical Industries, Ltd.) (1×10^5 cells/well) were seeded on the insert polyethylene terephthalate membrane, and 500 μL of DMEM-F12 (Sigma) with 20% of the three CMs was, respectively, poured into the tissue culture 24-well plate. SHSY5Y cells were derived from a neural crest tumor of early childhood, predominantly composed of undifferentiated neuroblast-like cells.[7] After 24 h, the SHSY5Y cells passing through the membrane were counted after detaching them with 0.05% trypsin–0.02% EDTA.

For cell proliferation assay, SHSY5Y cells (1×10^3/96-well plate) were cultured in DMEM-F12 containing 10% FBS for 24 h, and subsequently in serum-free DMEM-F12 containing 0.2% bovine serum albumin for further 24 h. Then, the medium was changed into each DMEM-F12 containing 0.02% FBS with 20% of three CMs. Ten micrometers of Tetra-color one (Seikagaku Kogyo, Co.) was added to the 96 well-plate, and cell numbers were measured by spectrophotometry at 450 nm at 2, 12, 24, 36, and 48 h of culture.

For the anti-apoptotic assay, SHSY5Y cells were cultured in DMEM-F12 in a 35-mm dish for 2 days and then incubated with 300 nM staurosporine[8] (Sigma) in DMEM-F12 with 20% of the three CMs. After 24 h, SHSY5Y were harvested, and

the cell suspensions were treated with Annexin V-FITC (Roche Diagnostics) and PI for 15 min, and analyzed by flow cytometry JSAN.

BDNF (Peprotech), GDNF (Peprotech), VEGF-A (Peprotech), or NGF (Peprotech) at 50 ng/mL was used as a control for the three assays.

Evaluation of motor disability

Rats were blindly examined on days 0, 2, 6, and 9 with a standardized motor disability scale by slight modifications.[9] Rats were scored 1 point for each of the following parameters: flexion of the forelimb contralateral to the stroke when instantly hung by the tail, extension of the contralateral hind limb when pulled from the table, and rotation to the paretic side against resistance. In addition, 1 point was scored for circling motion to the paretic side when trying to walk, 1 point was scored for failure to walk out of a circle of 50 cm in diameter within 10 s, 2 points were scored for failure to leave the circle within 20 s, and 3 points were scored for inability to exit the circle within 60 s. In addition, 1 point each was scored for inability of the rat to extend the paretic forepaw when pushed against the table from above, laterally, and sideways. The motor disability scale was performed 3 times per animal time-point.

Assessment of infarct volume

The cryosections obtained from samples on days 3 and 21 were stained with hematoxylin and eosin.[10] ImageJ (National Institutes of Health) was used to determine each infarct area in 9 coronal sections in 12-μm thickness at 0.84-mm intervals. All of the infarction area was covered by these nine coronal sections. Regional infarct volumes were calculated by summing the infarct areas and multiplying these areas by the distance between sections (0.84 mm), followed by remediation for brain edema.[11]

Statistical analyses

Data are reported as means ± SD. p-Values were calculated using the unpaired Student's t-test.

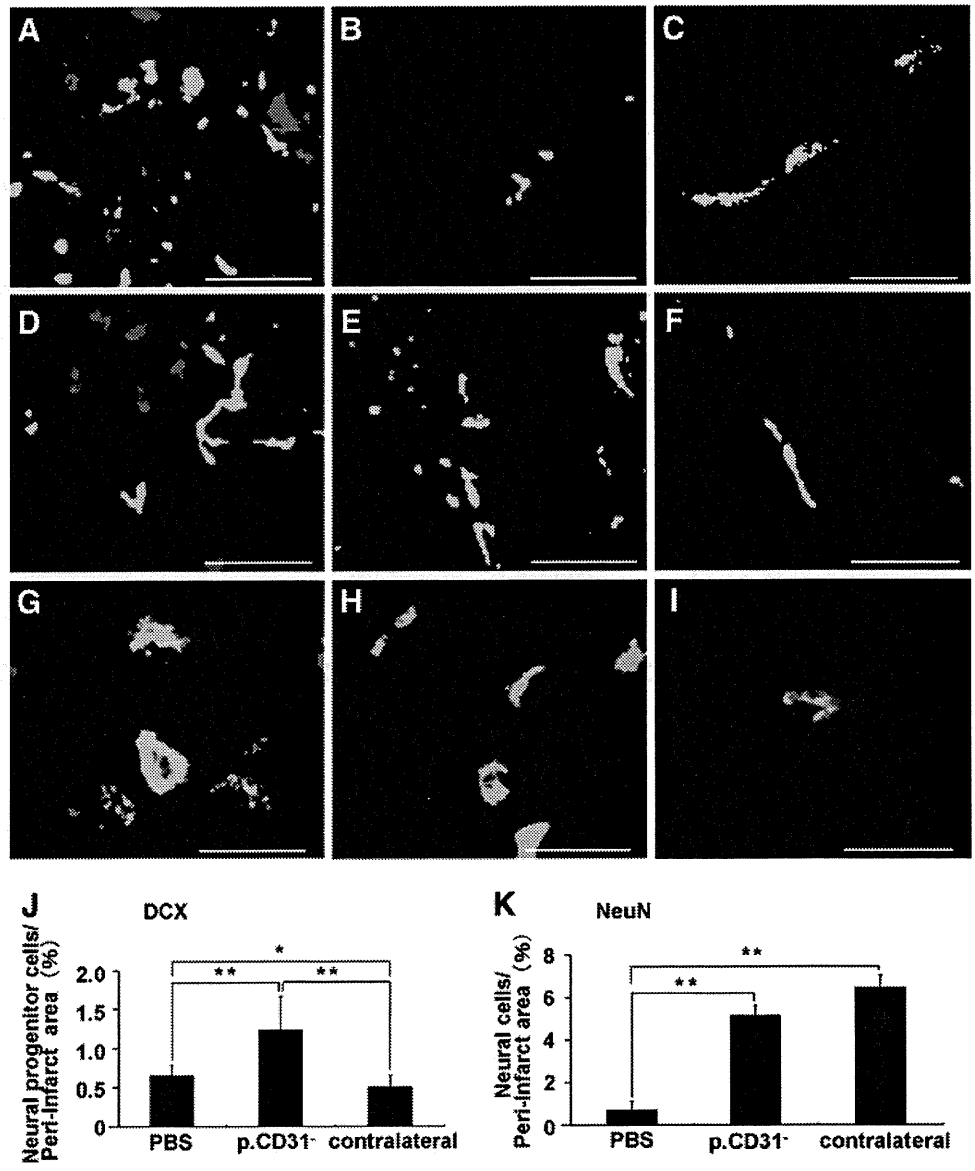

FIG. 2. Doublecortin-positive cells (green: **A–C**), Neurofilament-positive cells (green: **D–F**), and NeuN-positive cells (green: **G–I**). $CD31^-/CD146^-$ SP cells (red) transplantation group of the ipsilateral **(A, D, G)** and the contralateral **(B, E, H)** on day 21. PBS group **(C, F, I)** on day 21. Statistical analyses of density of NPCs **(J)** and neurons **(K)** on day 21. Scale bars = 20 μm. $^*p < 0.005$, $^{**}p < 0.001$, Student's t-test. Each point is expressed as mean ± SD of 75 determinations. NPC, neuronal progenitor cells; PBS, phosphate-buffered saline. Color images available online at www.liebertonline.com/tea

Results

Pulp stem cell outcome

DiI-labeled transplanted $CD31^-/CD146^-$ SP cells were characterized by round-to-oval nuclei with minimal variable cytoplasm. The transplanted cells survived and migrated from the original injection site to peri-infarct area in the cortex and striatum (Fig. 1D).

Transplanted cells localized in proximity of doublecortin (Fig. 2A) and neurofilament (Fig. 2D) or NeuN-positive cells (Fig. 2G) on day 21. Few doublecortin cells were observed in the contralateral side (Fig. 2B). There was a twofold increase in doublecortin-positive cells (Fig. 2J) and an eightfold increase in NeuN-positive cells (Fig. 2K) on day 21 in the $CD31^-/CD146^-$ SP cell transplantation group compared with that in the PBS group. No evidence of differentiation of $CD31^-/CD146^-$ SP cells into neurons or endothelial cells was detected. The migration of NPCs with doublecortin from SVZ to the peri-infarct area was observed on days 9 and 21. The migration on day 9 was more prominent (Fig. 3I, K, M). These results suggest that the transplanted cells support the migration and differentiation of the NPCs. The number of

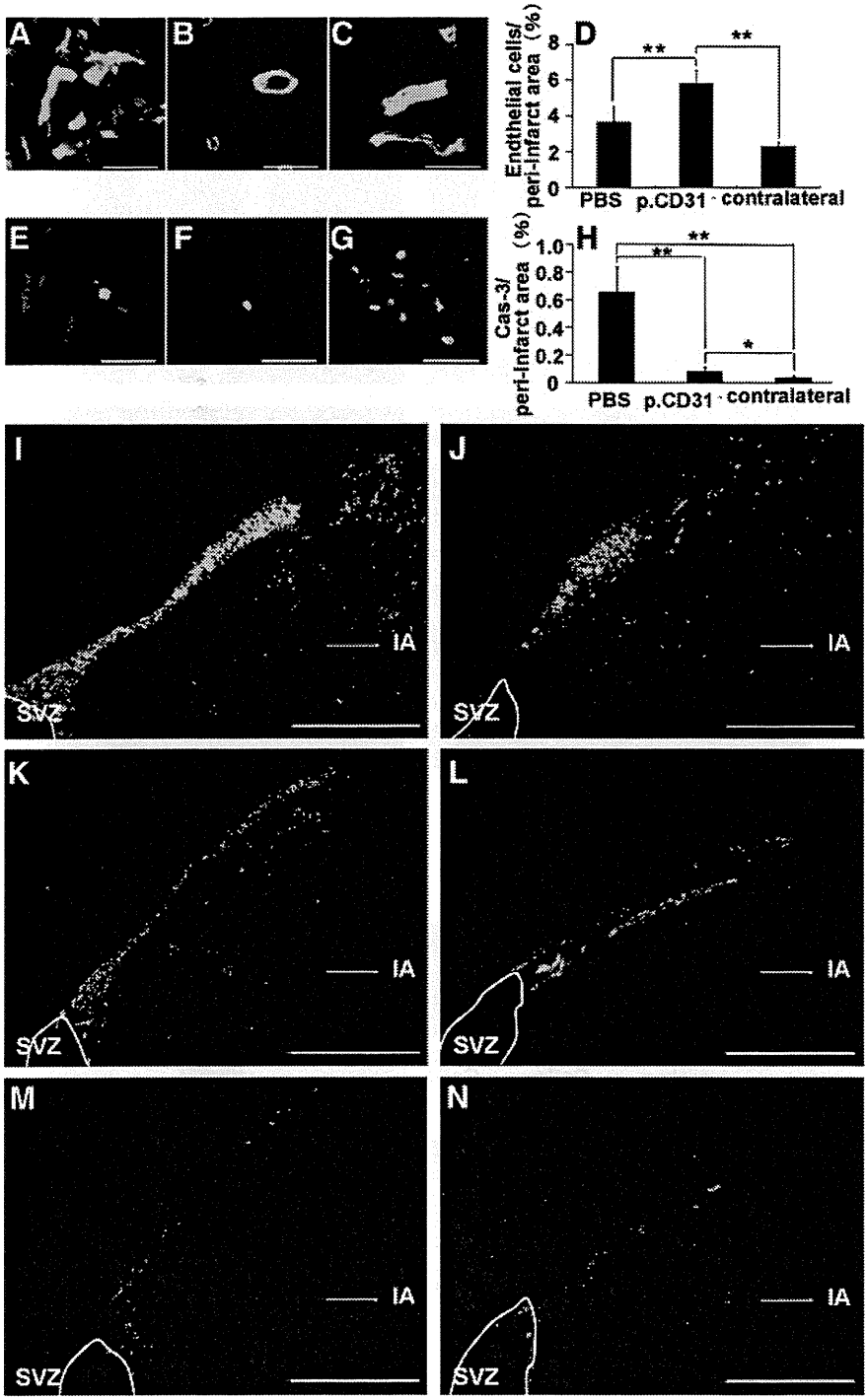

FIG. 3. RECA1-positive cells on day 21 (green: **A–C**) and cleaved caspase-3-positive cells on day 3 (green: **E–G**). $CD31^-/CD146^-$ SP cells (red) transplantation group of the ipsilateral **(A, E)** and the contralateral **(B, F)**. PBS group **(C, G)**. Statistical analyses of density of endothelial cells on day 21 **(D)** and cleaved caspase-3-positive cell on day 3 **(H)**. The migration of NPC from the SVZ to the peri-infarct area on days 9 **(I, J, M)** and 21 **(K, L, N)**. $CD31^-/CD146^-$ SP cells group **(I, J)**. Unfractionated pulp cells **(K, L)**. PBS group **(M, N)**. Scale bar = 20 μm **(A–C, E–G)**, and 300 μm **(I–N)**. $^*p < 0.01$, $^{**}p < 0.001$, Data were expressed as means ± SD at 75 determinations. The statistical difference was calculated by Student's *t*-test. IA, infarct area; SVZ, subventricular zone. Color images available online at www.liebertonline.com/tea

RECA1-positive cells on day 21 was increased in the CD31$^-$/CD146$^-$ SP cell transplantation group compared with that in the PBS group (Fig. 3D), indicating that the transplanted cells also promote angiogenesis after ischemia. In the CD31$^-$/CD146$^-$ SP cell transplantation group (Fig. 3H), there was a decrease in cleaved caspase-3-positive cells, suggesting that the transplanted cells have an anti-apoptotic function.

Expression of neurotrophic factors

The expression of several neurotrophic factors *VEGF*, *GDNF*, *NGF*, and *BDNF* was detected with *in situ* hybridization in the DiI-labeled CD31$^-$/CD146$^-$ SP cells in the peri-infarct area on day 21 (Fig. 4A–D). Real-time RT-PCR analysis demonstrated that expression of *VEGF* mRNA by the transplanted CD31$^-$/CD146$^-$ SP cells in the ischemic region on day 21 was 1,000 times and 28 times higher than that of normal porcine brain and that of the transplanted CD31$^-$/CD146$^-$ SP cells into normal rat striatum, respectively (Fig. 4E, F). Immunohistochemistry of VEGF showed that the VEGF protein was highly expressed in the DiI-labeled CD31$^-$/CD146$^-$ SP cells in the peri-infarct area on day 3 (Fig. 4G) compared with that on day 21 (Fig. 4H).

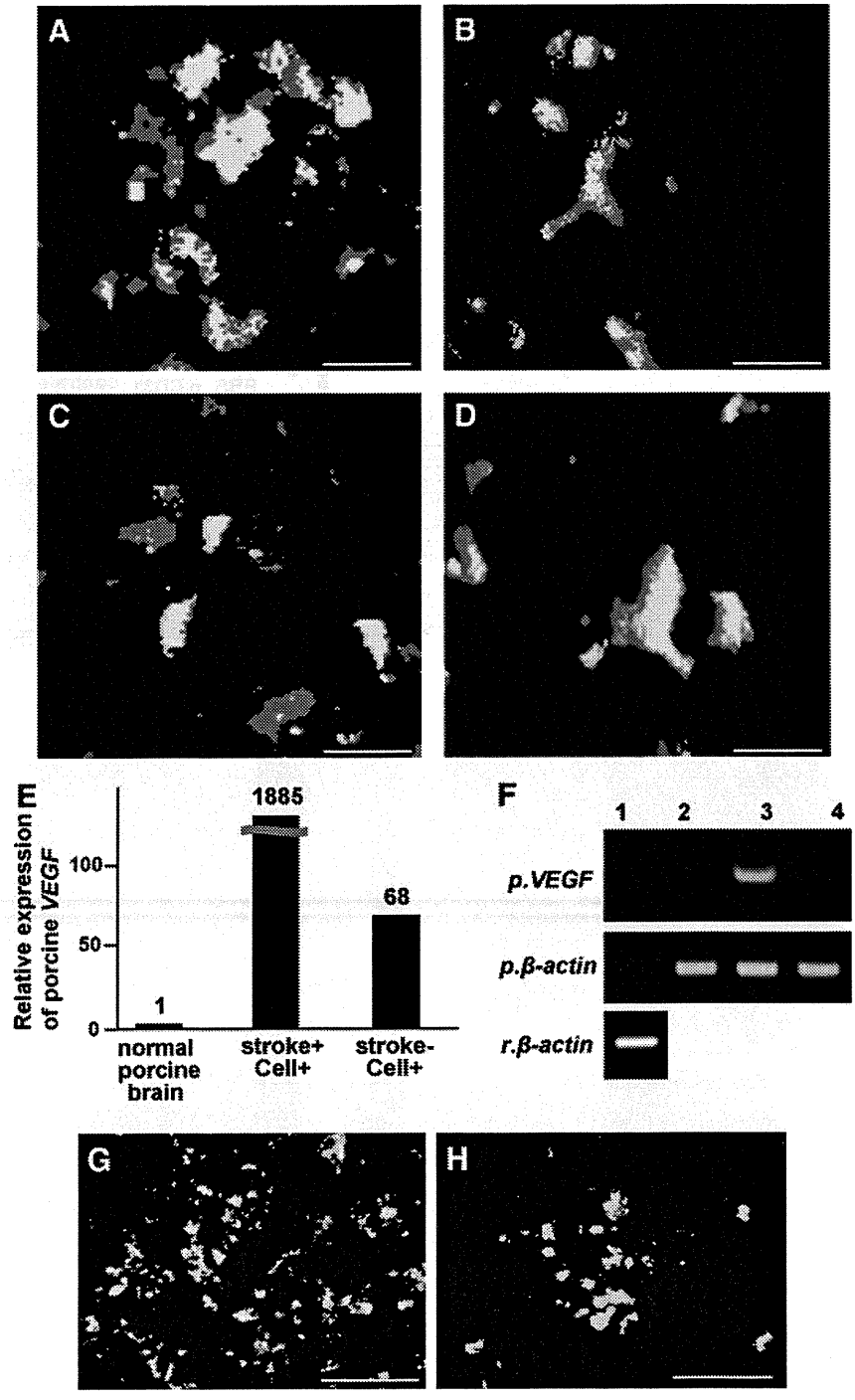

FIG. 4. Analysis of expression of *VEGF* **(A)**, *GDNF* **(B)**, *BDNF* **(C)**, and *NGF* **(D)** (green: **A–D)** of DiI-labeled transplanted CD31$^-$/CD146$^-$ SP cells (red) by *in situ* hybridization in the peri-infarct area. Real-time reverse transcription–polymerase chain reaction analysis of porcine *VEGF* (*pVEGF*) using porcine-specific primers **(E)**. Expression of porcine *VEGF* and porcine-specific and rat-specific β-actin 1, normal rat brain; 2, normal porcine brain; 3, peri-infarct area 21 days after transplantation of CD31$^-$/CD146$^-$ SP cells; 4, normal rat striatum 21 days after transplantation of the cells **(F)**. VEGF-positive cells on day 3 **(G)** and on day 21 **(H)** by immunohistochemistry. Scale bars = 10 μm **(A–D)** and 100 μm **(G, H)**. BDNF, brain-derived neurotrophic factor; GDNF, glial cell line-derived neurotrophic factor; NGF, nerve growth factor; VEGF, vascular endothelial growth factor. Color images available online at www.liebertonline.com/tea

Migration, proliferation, and anti-apoptotic assays

CM of CD31$^-$/CD146$^-$ SP cells showed higher migratory effect on SHSY5Y cells than VEGF, NGF, and BDNF, and was similar to GDNF (Fig. 5A). Its proliferation effect was higher than VEGF and NGF, and similar to BDNF and GDNF (Fig. 5B). Its anti-apoptotic activity was higher than BDNF, GDNF, and VEGF (Fig. 5C).

Evaluation of motor function

All groups (CD31$^-$/CD146$^-$ SP cells, unfractionated pulp cells, and PBS) displayed high score for motor function at the early stage (day 0, scores are 8.08±0.79; 8.25±0.96; 8.42±0.79, and day 2, 5.08±0.90; 6.25±1.26; 7.67±0.78, respectively). Progressive improvement in motor disability in the CD31$^-$/CD146$^-$ SP cell transplantation group after day 2 became significant on day 6 compared with PBS control group (2.67±1.23; 6.83±0.72), and more significant on day 9 compared with the unfractionated pulp cells and the PBS control group (1.33±0.78; 2.8±0.96; 6.50±0.67) (Fig. 6A). Persistent improvement in CD31$^-$/CD146$^-$ SP cells transplantation group was noted on day 14 (1.00±0.71) and 21 (0.80±0.45), whereas persistent impairment of motor disability (score above 4) was observed in the PBS group on day 14 (5.60±0.55) and 21 (5.40±0.59) (Fig. 6A). Further, the video image demonstrated significant recovery in motor function of the CD31$^-$/CD146$^-$ SP cell transplantation group compared with the unfractionated pulp cells and PBS control groups on day 6 (Supplementary Videos S1–S3; Supplementary Data are available online at www.liebertonline.com/tea).

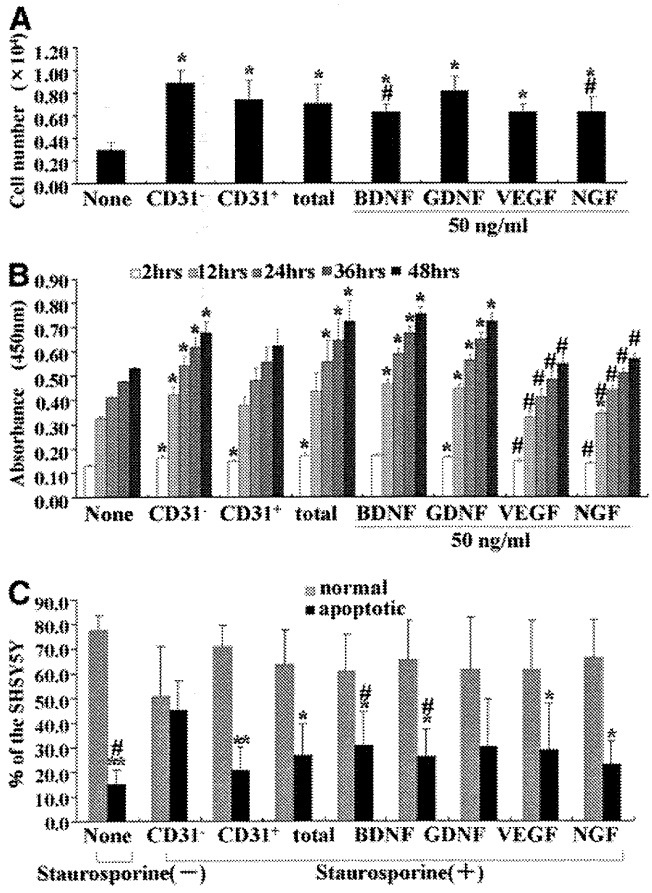

FIG. 5. The migration **(A)**, proliferative effect **(B)**, and anti-apoptotic effect **(C)** of conditioned medium of CD31$^-$/CD146$^-$ SP cells, CD31$^+$/CD146$^-$ SP cells, and unfractionated total pulp cells and neurotrophic factors on SHSY5Y cells. $^*p<0.05$, $^{**}p<0.005$, versus control. $^{\#}p<0.05$, versus CD31$^-$/CD146$^-$ SP cells. Data were expressed as means±SD at three determinations **(A, C)** and four determinations **(B)**. Student's *t*-test.

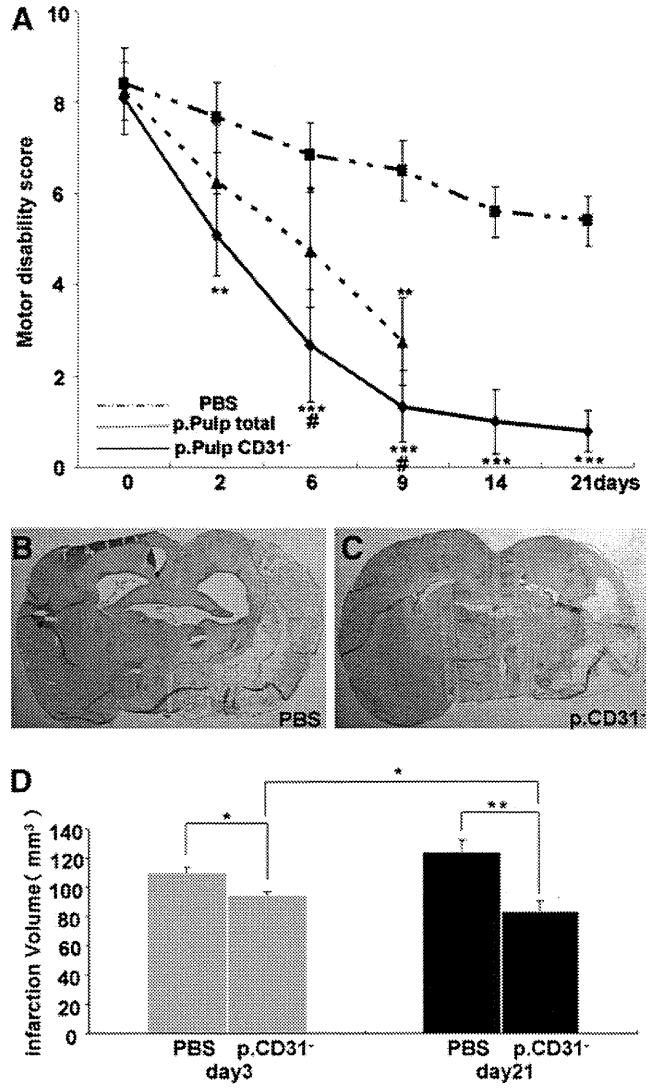

FIG. 6. Motor disability test by injection of the CD31$^-$/CD146$^-$ SP cells, the unfractionated pulp cells and the PBS on days 0, 2, 6, and 9 **(A)**. Infarct area on day 21 **(B, C)**. The reduction of the infarct volume 3 and 21 days after injection of CD31$^-$/CD146$^-$ SP cells **(D)**. $^*p<0.05$, $^{**}p<0.005$, $^{***}p<0.001$, versus control. $^{\#}p<0.05$, versus CD31$^-$/CD146$^-$ SP cells. Data were expressed as means±SD at three determinations **(D)**, Student's *t*-test.

Reduction of infarct volume

There was a significant decrease in the infarct volume on days 3 and 21 in the CD31$^-$/CD146$^-$ SP cell transplantation

group (day 3, $95.2 \pm 2.5\,mm^3$, $n=3$: day 21, $84.7 \pm 6.5\,mm^3$, $n=4$) compared to PBS group (day 3, $109.7 \pm 4.1\,mm^3$, $n=3$: day 21, $123.9 \pm 7.4\,mm^3$, $n=4$). The difference of infarct volume between the $CD31^-/CD146^-$ SP cell transplantation group and the PBS group increased over time (reduced by 13.3% on day 3 and reduced by 32.9% on day 21) (Fig. 6D). These results suggest that transplanted $CD31^-/CD146^-$ SP cells promoted the regeneration.

Discussion

In the current study, we demonstrated that transplanted $CD31^-/CD146^-$ SP cells migrated to the peri-infarct area. In addition, these cells released neurotrophic factors, and promoted migration and differentiation of the endogenous NPCs in SVZ. They also induced vasculogenesis in the peri-infarct area. These results indicate that $CD31^-/CD146^-$ SP cells ameliorated the ischemic tissue injury and accelerated the functional recovery after TMCAO. We have hypothesized that three mechanisms may contribute to the actions of VEGF. First, VEGF produced by transplanted cells may promote neurogenesis. NPCs in SVZ are known to migrate to the peri-infarct area and differentiate into neurons.[1] In this study, VEGF induced a chemotactic response in SHSY5Y cells. The transplanted $CD31^-/CD146^-$ SP cells migrated to the peri-infarct area and expressed VEGF. These results suggest that VEGF released by $CD31^-/CD146^-$ SP cells in the peri-infarct may promote migration of the endogenous NPCs in SVZ. Second, VEGF produced by transplanted cells may promote vasculogenesis. VEGF binds to its receptors on locally present vascular endothelial cells and directly initiates the angiogenic response.[12] In this study, the number of RECA1-positive endothelial cells significantly increased in the cell transplantation group. Third, VEGF may provide a neuroprotective effect. The neuroprotective effects of VEGF in experimental cerebral ischemia have been reported.[13] In cell the transplantation group, the number of cleaved caspase-3-immunopositive cells in the peri-infarct area was decreased compared with that in the PBS group, thus demonstrating the anti-apoptotic effects of VEGF on SHSY5Y cells. These results suggest that VEGF produced by $CD31^-/CD146^-$ SP cells may inhibit apoptosis of neurons. Thus, VEGF demonstrates pleiotropic effects on neurogenesis, vasculogenesis, and neuroprotection.

As VEGF is a potent vascular permeability factor, it may accelerate brain edema after stroke. Administration of VEGF in early ischemia (1 h after ischemia) leads to significant increase in blood–brain barrier leakage as well as enlarged ischemic areas.[14] However, VEGF administration at 24 h after TMCAO reduces infarct size, improves neurologic recovery, enhances neurogenesis in the SVZ and angiogenesis in the ischemic border zone.[14] In this study, $CD31^-/CD146^-$ SP cells were transplanted 24 h after TMCAO and we monitored the reduction of infarct size and improvement of motor disability. The time of administration of cells is critical. Thus, if $CD31^-/CD146^-$ SP cells were transplanted during an optimal window of time, they exhibit beneficial effects without the deleterious effects of edema.

In addition, $CD31^-/CD146^-$ SP cells expressed other neurotrophic factors such as GDNF,[15] NGF,[16] and *BDNF*[16] in the peri-infarct area. These neurotrophic factors had migratory, proliferative, and/or anti-apoptotic effects on SHSY5Y cells *in vitro* and may also contribute to the recovery from ischemic brain injury.

Finally, we explored the plausible underlying mechanisms of how injection of $CD31^-/CD146^-$ SP cells into the brains of immunocompetent rats staved off graft rejection. Blood–brain barrier is known to play a critical role in maintaining the immune-privileged status of the central nervous system.[17] It is well known that mesenchymal stem cells from bone marrow are not rejected by hosts and immunosuppression is not required in rodents.[1] Dental pulp stem cells have many similarities to mesenchymal stem cells; transplanted $CD31^-/CD146^-$ SP cells possess immunosuppressive properties.[18]

Conclusion

In summary, the transplantation of porcine $CD31^-/CD146^-$ SP cells promotes neurogenesis and vasculogenesis in an induced peri-infarct area, and enhances recovery after TMCAO in rats. Further research is needed to understand the underlying mechanisms. For potential clinical application and translational studies, the safety of $CD31^-/CD146^-$ SP cells must be assessed, including tumor formation. In conclusion, regeneration therapy using $CD31^-/CD146^-$ SP cells is a potential candidate in the treatment of stroke.

Acknowledgments

The authors thank Drs. Masataka Ito, Kayo Adachi, and Kiyomi Imabayasghi for their assistance. This work was supported by funds from Collaborative Development of Innovative Seeds, Potentiality verification stage from Japan Science and Technology Agency, a Grant-in-Aid for Scientific Research from the Ministry of Education, Science, Sports and Culture, Japan, No. 19659499 (M.N.), No. 20390504 (M.N.), and No. 18592173 (H.H.), and the Research Grant for Longevity Sciences (19C-2, 21A-7) from the Ministry of Health, Labour, and Welfare (M.N.).

Disclosure Statement

No competing financial interests exist.

References

1. Burns, T.C., Verfaillie C.M., and Low W.C. Stem cells for ischemic brain injury: a critical review. J Comp Neurol **515,** 125, 2009.
2. Locatelli, F., Bersano, A., Ballabio, E., Lanfranconi, S., Papadimitriou, D., Strazzer, S., Bresolin, N., Comi, G.P., and Corti, S. Stem cell therapy in stroke. Cell Mol Life Sci **66,** 757, 2009.
3. Gage, F.H., Kempermann, G., Palmer, T.D., Peterson, D.A., and Ray, J. Multipotent progenitor cells in the adult dentate gyrus. J Neurobiol **36,** 249, 1998.
4. Yang, K.L., Chen, M.F., Liao, C.H., Pang, C.Y., and Lin, P.Y. A simple and efficient method for generating Nurr1-positive neuronal stem cells from human wisdom teeth (tNSC) and the potential of tNSC for stroke therapy. Cytotherapy **11,** 606, 2009.
5. Iohara, K., Zheng, L., Wake, H., Ito, M., Nabekura, J., Wakita, H., Nakamura, H., Into, T., Matsushita, K., and Nakashima, M. A novel stem cell source for vasculogenesis in ischemia: subfraction of side population cells from dental pulp. Stem Cells **26,** 2408, 2008.

6. Longa, E.Z., Weinstein, P.R., Carlson, S., and Cummins, R. Reversible middle cerebral artery occlusion without craniectomy in rats. Stroke **20,** 84, 1989.
7. Koning, G., Colin, L., and Beyreuther, K. Retionic acid induced differentiated neuroblastoma cells show increased expression of the βA4 amyloid gene of Alzheimer's disease and an altered splicing pattern. FEBS Lett **269,** 305, 1990.
8. Richard, B., Eric, S., Patrick, O., Kurt, W., and Ywes, P. Induction of a common pathway of apoptosis by staurosporine. Exp Cell Res **211,** 314, 1994.
9. Leker, R.R., Gai, N., Mechoulam, R., and Ovadia, H. Drug-induced hypothermia reduces ischemic damage: effects of the cannabinoid HU-210. Stroke **34,** 2000, 2003.
10. Ginsberg, M.D. Adventures in the pathophysiology of brain ischemia: penumbra, gene expression, neuroprotection: the 2002 Thomas Willis Lecture. Stroke **34,** 214, 2003.
11. Leach, M.J., Swan, J.H., Eisenthal, D., Dopson, M., and Nobbs, M. BW619C89, a glutamate release inhibitor, protects against focal cerebral ischemic damage. Stroke **24,** 1063, 1993.
12. Plate, K.H., Beck, H., Danner, S., Allegrini, P.R., and Wiessner, C. Cell type specific upregulation of vascular endothelial growth factor in an MCA-occlusion model of cerebral infarct. J Neuropathol Exp Neurol **58,** 654, 1999.
13. Jin, K.L., Mao, X.O., and Greenberg, D.A. Vascular endothelial growth factor: direct neuroprotective effect in *in vitro* ischemia. Proc Natl Acad Sci U S A **97,** 10242, 2000.
14. Heike, B., and Karl, H.P. Angiogenesis after cerebral ischemia. Acta Neuropathol **117,** 481, 2009.
15. Leu-Fen, H., Lin, H., Doherty, D., Lile, B., and Frank, C. GDNF: a glial cell line-derived neurotrophic factor for midbrain dopaminergic neurons. Science **260,** 1072, 1993.
16. Shawne, N., Fernando, G., James, C., and Carl, C. Physical activity increases mRNA for brain-derived neurotrophic factor and nerve growth factor in rat brain. Brain Res **726,** 49, 1996.
17. Pachter, J.S., De Vries, H.E., and Fabry, Z. The blood-brain barrier and its role in immune privilege in the central nervous system. J Neuropathol Exp Neurol **62,** 593, 2003.
18. Pierdomenico, L., Bonsi, L., Calvitti, M., Rondelli, D., Arpinati, M., Chirumbolo, G., Becchetti, E., Marchionni, C., Alviano, F., Fossati, V., Staffolani, N., Franchina, M., Grossi, A., and Bagnara, G.P. Multipotent mesenchymal stem cells with immunosuppressive activity can be easily isolated from dental pulp. Transplantation **80,** 836, 2005.

Address correspondence to:
Misako Nakashima, Ph.D.
Department of Oral Disease Research
National Center for Geriatrics and Gerontology
Research Institute
35 Gengo, Morioka, Obu
Aichi 474-8522
Japan

E-mail: misako@ncgg.go.jp

Received: May 24, 2010
Accepted: January 10, 2011
Online Publication Date: February 22, 2011

Supplementary Data

SUPPLEMENTARY VIDEO S1. $CD31^-/CD146^-$ SP cell transplantation on day 6.

SUPPLEMENTARY VIDEO S2. Unfractionated pulp cell transplantation on day 6.

SUPPLEMENTARY VIDEO S3. PBS injection on day 6.

Research article

Human dental pulp-derived stem cells promote locomotor recovery after complete transection of the rat spinal cord by multiple neuro-regenerative mechanisms

Kiyoshi Sakai,[1] Akihito Yamamoto,[1] Kohki Matsubara,[1] Shoko Nakamura,[1] Mami Naruse,[1] Mari Yamagata,[1] Kazuma Sakamoto,[2] Ryoji Tauchi,[3] Norimitsu Wakao,[3] Shiro Imagama,[3] Hideharu Hibi,[1] Kenji Kadomatsu,[2] Naoki Ishiguro,[3] and Minoru Ueda[1]

[1]Department of Oral and Maxillofacial Surgery, [2]Department of Biochemistry, and
[3]Department of Orthopedic Surgery, Nagoya University Graduate School of Medicine, Nagoya, Japan.

Spinal cord injury (SCI) often leads to persistent functional deficits due to loss of neurons and glia and to limited axonal regeneration after injury. Here we report that transplantation of human dental pulp stem cells into the completely transected adult rat spinal cord resulted in marked recovery of hind limb locomotor functions. Transplantation of human bone marrow stromal cells or skin-derived fibroblasts led to substantially less recovery of locomotor function. The human dental pulp stem cells exhibited three major neuroregenerative activities. First, they inhibited the SCI-induced apoptosis of neurons, astrocytes, and oligodendrocytes, which improved the preservation of neuronal filaments and myelin sheaths. Second, they promoted the regeneration of transected axons by directly inhibiting multiple axon growth inhibitors, including chondroitin sulfate proteoglycan and myelin-associated glycoprotein, via paracrine mechanisms. Last, they replaced lost cells by differentiating into mature oligodendrocytes under the extreme conditions of SCI. Our data demonstrate that tooth-derived stem cells may provide therapeutic benefits for treating SCI through both cell-autonomous and paracrine neuroregenerative activities.

Introduction

The development of effective treatments for spinal cord injury (SCI) has been stifled by this injury's complicated pathophysiology (1). During the acute phase, the focal mechanical insult disrupts tissue homeostasis. This triggers secondary injury processes in which multiple destructive cascades cause the necrotic and apoptotic death of neurons, astrocytes, and oligodendrocytes, which spreads beyond the initial injury site and leads to irreversible axonal damage and demyelination (2, 3). Subsequently, reactive astrocytes and oligodendrocytes near the site of injured spinal cord (SC) respectively produce chondroitin sulfate proteoglycans (CSPGs) and myelin proteins (including myelin-associated glycoprotein [MAG], Nogo, oligodendrocyte myelin glycoprotein [OMgp], netrin, semaphorin, and ephrin). These extracellular molecules function as axon growth inhibitors (AGIs), acting through the intracellular Rho GTPase signaling cascade (4). These multiple pathogenic signals synergistically accelerate the progressive deterioration after SCI. Therefore, therapeutic strategies for functional recovery from SCI must exert multifaceted reparative effects against a variety of pathogeneses (2).

Stem cell–based transplantation therapy holds great promise for establishing such a multifaceted therapeutic strategy. In the last decade, a variety of cell types, including human neural stem cells (5), embryonic stem cell derivatives (6–8), and adult bone marrow stromal cells (BMSCs) (9, 10), have been transplanted into the injured SC of rats or mice, and their neuroregenerative activities evaluated. These preclinical studies showed that engrafted stem cells promote substantial functional recovery after SCI through both cell-autonomous/cell-replacement and paracrine/trophic effects (11). However, the previously tested stem cells show poor survival (6–8, 12) and/or differentiation under the severe conditions of SCI (9, 13, 14), and the transplantation of individual stem cells has led to only modest therapeutic benefits. Furthermore, although the trophic factors derived from these stem cells promote in vitro neurite extension and survival, their roles in the functional recovery of SCI are still largely unknown.

Human adult dental pulp stem cells (DPSCs) and stem cells from human exfoliated deciduous teeth (SHEDs) are self-renewing stem cells residing within the perivascular niche of the dental pulp (15). They are thought to originate from the cranial neural crest and express early markers for both mesenchymal and neuroectodermal stem cells (16, 17). Since naturally exfoliated deciduous and impacted adult wisdom teeth are not usually needed, DPSCs and SHEDs can be obtained without adverse health effects. Similar to BMSCs, these cells are able to differentiate into osteoblasts, chondrocytes, adipocytes, endothelial cells, and functionally active neurons in vitro, under defined conditions (16–19). Trophic factors expressed by them promote neuronal survival, proliferation, differentiation, and migration (20–23). Thus, these previous reports support the use of tooth-derived stem cells as a unique cellular resource for neuroregeneration therapies. However, their ability to promote functional recovery in neurological disorders remains largely unknown.

Authorship note: Kiyoshi Sakai and Akihito Yamamoto contributed equally to this work.

Conflict of interest: The authors have declared that no conflict of interest exists.

Citation for this article: *J Clin Invest* doi:10.1172/JCI59251.

Table 1
Flow cytometry of stem cells from humans

	SHEDs ($n = 3$)		DPSCs ($n = 3$)		BMSCs ($n = 3$)	
	Positive (%)	SD	Positive (%)	SD	Positive (%)	SD
MSC markers						
CD90	98.25	0.91	98.96	0.95	≥90	
CD73	91.45	8.44	96.60	2.14	≥90	
CD105	98.20	2.44	98.23	0.54	≥90	
Negative markers						
CD45	0.33	0.28	0.11	0.09	≤10	
CD34	0.36	0.32	0.07	0.03	≤10	
CD11b	0.02	0.02	0.03	0.02	≤10	
HLA-DR	0.45	0.39	0.12	0.10	≤10	
Neural markers						
DCX	95.42	0.66	84.45	0.45	91.37	8.20
Nestin	92.71	10.46	95.40	1.52	35.76	8.06
GFAP	92.93	8.30	97.50	3.54	4.49	3.11
βIII-Tubulin	99.69	0.21	85.43	0.77	99.24	0.73
NeuN	31.93	7.25	26.61	4.28	2.97	1.74
A2B5	94.84	3.72	96.34	0.33	35.47	15.07
CNPase	99.21	0.11	98.19	0.46	21.35	7.81
APC	0.20	0.01	0.36	0.02	2.75	2.05
MBP	0.68	0.04	0.32	0.02	3.02	2.00

Here we examined the neuroregenerative activities of DPSCs and SHEDs by transplanting them into a completely transected rat SCI model during the acute phase, in which axonal regeneration rather than axonal sprouting can be evaluated accurately. Our data show that these tooth-derived stem cells promoted functional recovery after SCI by multifaceted neuro-regenerative activities, via both cell-autonomous/cell replacement and paracrine/trophic mechanisms.

Results

Characterization of isolated human SHEDs and DPSCs for use in transplantation studies. Flow cytometry analysis showed that the SHEDs and DPSCs expressed a set of mesenchymal stem cell (MSC) markers (i.e., CD90, CD73, and CD105), but not endothelial/hematopoietic markers (i.e., CD34, CD45, CD11b/c, and HLA-DR) (Table 1). Like human BMSCs, both the SHEDs and DPSCs exhibited adipogenic, chondrogenic, and osteogenic differentiation as described previously (refs. 16, 17, and data not shown). The majority of SHEDs and DPSCs coexpressed several neural lineage markers: nestin (neural stem cells), doublecortin (DCX; neuronal progenitor cells), βIII-tubulin (early neuronal cells), NeuN (mature neurons), GFAP (neural stem cells and astrocytes), S-100 (Schwann cells), and A2B5 and CNPase (oligodendrocyte progenitor cells), but not adenomatous polyposis coli (APC) or myelin basic protein (MBP) (mature oligodendrocytes) (Figure 1A and Table 1). This expression profile was confirmed by immunohistochemical analyses (Figure 1B).

Next, we examined the expression of representative neurotrophic factors by real-time PCR. Both the SHEDs and DPSCs expressed glial cell–derived neurotrophic factor (*GDNF*), brain-derived neurotrophic factor (*BDNF*), and ciliary neurotrophic factor (*CNTF*) at more than 3 to 5 times the levels expressed by skin-derived fibroblasts or BMSCs (Figure 1C).

We further characterized the transcriptomes of SHEDs and BMSCs by cDNA microarray analysis. This gene expression analysis revealed a 2.0-fold difference in the expression of 3,318 of 41,078 genes between SHEDs and BMSCs. Of these, 1,718 genes were expressed at higher levels in the SHEDs and 1,593 genes were expressed at lower levels (data not shown). The top 30 genes showing higher expression in the SHEDs were in the following ontology categories: extracellular and cell surface region, cell proliferation, and tissue/embryonic development (Table 2).

SHEDs and DPSCs promoted locomotor recovery after SCI. To compare the neuroregenerative activities of human SHEDs and DPSCs with those of human BMSCs and human skin fibroblasts, we transplanted the cells into the completely transected SCs, as described in Methods, and evaluated locomotion recovery using the Basso, Beattie, Bresnahan locomotor rating scale (BBB scale) (24). Remarkably, the animals that received SHEDs or DPSCs exhibited a significantly higher BBB score during the entire observation period, compared with BMSC-transplanted, fibroblast-transplanted, or PBS-injected control rats (Figure 2A). Importantly, their superior recoveries were evident soon after the operation, during the acute phase of SCI. After the recovery period (5 weeks after the operation), the rats that had received SHEDs were able to move 3 joints of hind limb coordinately and walk without weight support ($P < 0.01$; Supplemental Videos 1 and 2), while the BMSC- or fibroblast-transplanted rats exhibited only subtle movements of 1–2 joints. These results demonstrate that the transplantation of SHEDs or DPSCs during the acute phase of SCI significantly improved the recovery of hind limb locomotor function. Since the level of recovery was similar in the SHED- and DPSC-transplanted rats, we focused on the phenotypical examination of SHED-transplanted rats to elucidate how tooth-derived stem cells promoted the regeneration of the completely transected rat SC.

SHEDs regenerated the transected corticospinal tract and raphespinal serotonergic axons. To examine whether engrafted SHEDs affect the preservation of neurofilaments, we performed immunohistochemical analyses with an anti-neurofilament M (NF-M) mAb, 8 weeks after transection. Compared with the PBS-treated control SCs, the SHED-transplanted SCs exhibited greater preservation of NF-positive axons from 3 mm rostral to 3 mm caudal to the transected lesion site (Figure 2, B and C; asterisk indicates epicenter). The percentages of NF-positive axons in the epicenter of the SHED-transplanted and control SCs were 35.8% ± 13.0% and 8.7% ± 3.4%, respectively, relative to sham-treated SCs (Figure 2D).

Regeneration of both the corticospinal tract (CST) and the descending serotonergic raphespinal axons is important for the recovery of hind limb locomotor function in rat SCI. We therefore examined whether these axons had extended beyond the epicenter in the SHED-transplanted SCs. The CST axons were traced with the anterograde tracer biotinylated dextran amine (BDA), which was injected into the sensorimotor cortex. The serotoner-

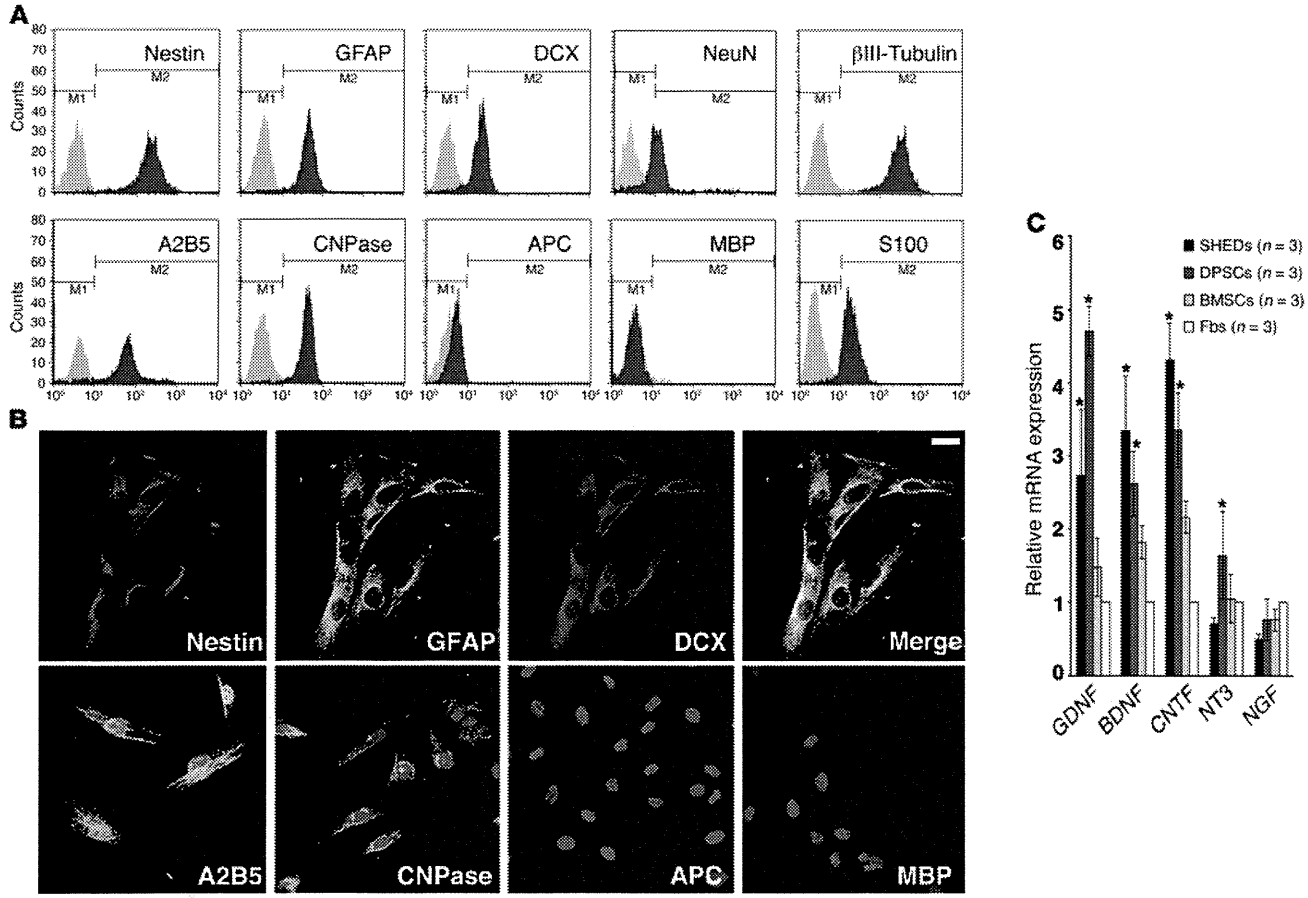

Figure 1

Characterization of the SHEDs and DPSCs used for transplantation. (**A**) Flow cytometry analysis of the neural cell lineage markers expressed in SHEDs. Note that most of the SHEDs and DPSCs coexpressed neural stem and multiple progenitor markers, but not mature oligodendrocytes (APC and MBP). (**B**) Confocal images showing SHEDs coexpressed nestin, GFAP, and DCX. SHEDs also expressed markers for oligodendrocyte progenitor cells (A2B5 and CNPase), but not for mature oligodendrocytes (APC and MBP). Scale bar: 10 μm. (**C**) Real-time RT-PCR analysis of the expression of neurotrophic factors. Results are expressed as fold increase compared with the level expressed in skin fibroblasts. Data represent the average measurements for each cell type from 3 independent donors. This set of experiments was repeated twice and yielded similar results. Data represent the mean ± SEM. $^*P < 0.01$ compared with BMSCs and fibroblasts (Fbs).

gic raphespinal axons were immunohistochemically detected by a mAb that specifically reacts with serotonin (5-hydroxytryptamine [5-HT]), which is synthesized within the brain stem. We found that both BDA- and 5-HT–positive fibers extended as far as 3 mm caudal to the epicenter in the SHED-transplanted but not the control group (Figures 3 and 4). Furthermore, some BDA- and 5-HT–positive boutons could be seen apposed to neurons in the caudal stump (Figure 3D and Figure 4C), suggesting that the regenerated axons had established new neural connections. Notably, although the number of descending axons extending beyond the epicenter was small, we observed many of them penetrating the scar tissue of the rostral stump (Figure 3A and Figure 4A). The percentages of 5-HT–positive axons of the SHED-transplanted SCs at 1 and 3 mm rostral to the epicenter were 58.9% ± 3.9% and 78.3% ± 7.4% relative to sham-treated SC, respectively (Figure 4D). These results demonstrate that the engrafted SHEDs promoted the recovery of hind limb locomotion via the preservation and regeneration of transected axons, even in the microenvironment of the damaged CNS.

SHEDs inhibited the Rho GTPase activity induced by SC transection. The apparent axon regeneration in the SHED-transplanted SCs suggested that the SHEDs might modulate multiple AGI signals generated from oligodendrocytes and reactive astrocytes forming the glial scar. We therefore measured the activity level of Rho GTPase, which is an intracellular target of multiple AGIs, by pull-down assay. The injured SCs were isolated 7 days after transection and subjected to immunoprecipitation with GST-tagged Rho-binding domain (RBD). The level of active Rho (GTP-bound Rho [GTP-Rho]) in the transected control SCs increased; however, the engrafted SHEDs remarkably inhibited the activation of Rho (Figure 4E). These results strongly suggest that SHEDs promoted axon regeneration through the inhibition of multiple AGI signals.

Serum-free conditioned medium from both SHEDs and DPSCs antagonizes CSPG- or MAG-mediated neurite growth inhibition. Next, to analyze the roles of trophic mechanisms in the SHED-mediated axon regeneration, we examined whether the conditioned medium (CM) from SHEDs (SHED-CM) or DPSCs (DPSC-CM) could promote the neurite extension of cerebral granular neurons (CGNs)

Table 2
Functional gene classification in SHEDs versus BMSCs

Term	Changed gene up	Total gene	P
Extracellular region	343	2,865	2.52×10^{-14}
Skeletal system development	104	661	1.46×10^{-9}
Extracellular matrix	101	678	9.20×10^{-9}
Extracellular space	147	1,134	2.00×10^{-8}
Extracellular matrix organization	43	195	4.86×10^{-8}
Multicellular organismal development	643	6,683	9.36×10^{-8}
Collagen fibril organization	20	57	4.97×10^{-7}
Anatomical structure morphogenesis	346	3,339	9.52×10^{-7}
Mitotic cell cycle	146	1,184	1.11×10^{-6}
Proteinaceous extracellular matrix	82	578	1.36×10^{-6}
Organ morphogenesis	144	1,182	2.43×10^{-6}
Vasculature development	98	732	3.76×10^{-6}
Embryonic morphogenesis	96	728	7.04×10^{-6}
Cell proliferation	245	2,288	7.17×10^{-6}
Cell cycle	230	2,135	9.74×10^{-6}
Blood vessel development	93	707	1.31×10^{-5}
Response to wounding	191	1,738	2.02×10^{-5}
Receptor protein serine/ threonine kinase signaling	56	369	2.12×10^{-5}
M phase of mitotic cell cycle	77	567	2.40×10^{-5}
Cell surface	86	671	3.26×10^{-5}
Organ development	362	3,675	3.68×10^{-5}
Collagen binding	21	90	3.90×10^{-5}
Glycosaminoglycan binding	42	262	4.65×10^{-5}
Mitotic spindle organization	12	33	7.15×10^{-5}
Cell adhesion	183	1,693	7.76×10^{-5}
Skeletal system morphogenesis	42	260	8.16×10^{-5}
Tissue development	185	1,720	8.76×10^{-5}
Cell surface receptor linked signaling pathway	368	3,785	8.98×10^{-5}
Mitosis	73	554	9.98×10^{-5}
Regulation of cell cycle	127	1,103	0.000109

on dishes coated with an AGI. CGNs isolated from newborn rats extended neurites on poly-L-lysine (PLL), but not on CSPG or MAG. Remarkably, both SHED-CM and DPSC-CM restored neurite extension activity of CGNs, while CM from fibroblasts (fibroblast-CM) or BMSCs (BMSC-CM) exhibited only subtle extension (Figure 5). Quantitative analysis showed that neurite extension through the inhibition of multiple AGIs was a unique characteristic of the tooth-derived stem cell (Figure 5, L and M). These results demonstrate that both SHEDs and DPSCs promote the regeneration of transected axons though direct inhibition of the multiple AGI signals by paracrine mechanisms.

SHEDs inhibited myelin degeneration. Next, we examined whether transplanted SHEDs preserved myelination in the transected SC by immunohistochemical staining with the fluorescent dye FluoroMyelin. In transverse sections of sham-operated SCs, white matter was clearly labeled by FluoroMyelin, and gray matter was not (data not shown). The control SCs exhibited little or no staining at the epicenter or 3 mm caudal to it (Figure 6, C and D). In contrast, we found significant FluoroMyelin-positive spots in the epicenter of the SHED-transplanted SCs, indicating that the SHEDs caused the regeneration of myelin structures in the transected region (Figure 6A). Notably, the myelin-positive areas of the SHED-transplanted SCs at 3 and 4 mm caudal to the epicenter constituted 55.3% ± 4.5% and 78.0% ± 4.1%, respectively, of the same areas in the sham-operated SCs, demonstrating that the SHEDs exerted remarkable myelin preservation activity (Figure 6E).

SHEDs survived and specifically differentiated into oligodendrocytes in the injured SC. In the FluoroMyelin-stained sections, we observed a myelin-expressing cell cluster in the gray matter of SHED-transplanted SCs (Figure 6B). We anticipated that these myelin-expressing cells would be mature oligodendrocytes derived from the transplanted SHEDs. To assess this possibility, we performed immunohistological analyses using anti-human nuclear antigen (HuNu) and two mature oligodendrocyte markers, APC and MBP (25, 26). Eight weeks after grafting, 32.3% ± 3.1% of the transplanted SHEDs still survived in the injured SCs (data not shown). Of these cells, 86.2% ± 6.2% and 90.2% ± 4.6% expressed APC and MBP, respectively (Figure 7). In addition, 10% of the HuNu-positive cells were negative for MBP and APC, but their fate is currently unknown (data not shown). Before the transplantation, SHEDs expressed many early neural cell lineage markers (Figure 1 and Table 1). However, the surviving transplanted SHEDs did not express NF-M or GFAP (Figure 7), indicating that they specifically differentiated along the oligodendrocyte lineage in the injured SCs.

SHEDs inhibited neuronal and glial apoptosis after SCI. SCI-induced cell death is a major contributor to secondary injury, in which irreversible tissue damage spreads across the SC. Twenty-four hours after injury, at 1 mm caudal to the epicenter, most of the cells expressing NeuN, GFAP, or MBP were costained with TUNEL, showing that massive multicellular apoptosis occurred immediately after SCI (Figure 8). The engrafted SHEDs significantly decreased the TUNEL staining in all 3 of these lineages (Figure 8, C, D, G, H, K, and L): The total number of TUNEL-positive cells in the SHED-transplanted SCs was approximately 20% of that in the control SCs (Figure 8M). The percentages of TUNEL-positive cells in the control and SHED-transplanted SCs were 87.7% ± 3.1% and 3.1% ± 3.2%, respectively (Figure 8N). These results demonstrate that the transplanted SHEDs minimized the expansion of secondary injury through strong neuroprotection of all the neural cell lineages.

Discussion

We report here the remarkable neuroregenerative activity of tooth-derived stem cells, SHEDs and DPSCs, for functional recovery after SCI. Previous studies have dealt with the differentiation characteristics of tooth-derived stem cells (16–19) and their trophic effects on the proliferation, migration, and survival of particular subsets of neurons (20–23). However, few studies have considered the therapeutic benefits of these stem cells for a particular neurological disorder. Our study revealed that engrafted SHEDs exhibited three major therapeutic benefits for recovery after SCI, including (a) inhibition of SCI-induced apoptosis of neurons, astrocytes, and oligodendrocytes, which promoted the preservation of neural fibers and myelin sheaths; (b) regeneration of the transected axon through the direct inhibition of multiple AGI signals, such as CSPGs and MAG,